SANDIA REPORT
SAND2005-7246
Unlimited Release
Printed November 2005

Piezoelectric Field in Strained GaAs

Sebastian M. Wieczorek and Weng W. Chow

Prepared by
Sandia National Laboratories
Albuquerque, New Mexico 87185 and Livermore, California 94550

Sandia is a multiprogram laboratory operated by Sandia Corporation,

a Lockheed Martin Company, for the United States Department of Energy's
National Nuclear Security Administration under Contract DE-AC04-94AL85000.

Approved for public release; further dissemination unlimited.

Sandia National Laboratories

Issued by Sandia National Laboratories, operated for the United States Department of Energy by Sandia Corporation.

NOTICE: This report was prepared as an account of work sponsored by an agency of the United States Government. Neither the United States Government, nor any agency thereof, nor any of their employees, nor any of their contractors, subcontractors, or their employees, make any warranty, express or implied, or assume any legal liability or responsibility for the accuracy, completeness, or usefulness of any information, apparatus, product, or process disclosed, or represent that its use would not infringe privately owned rights. Reference herein to any specific commercial product, process, or service by trade name, trademark, manufacturer, or otherwise, does not necessarily constitute or imply its endorsement, recommendation, or favoring by the United States Government, any agency thereof, or any of their contractors or subcontractors. The views and opinions expressed herein do not necessarily state or reflect those of the United States Government, any agency thereof, or any of their contractors.

Printed in the United States of America. This report has been reproduced directly from the best available copy.

Available to DOE and DOE contractors from
U.S. Department of Energy
Office of Scientific and Technical Information
P.O. Box 62
Oak Ridge, TN 37831

Telephone: (865)576-8401
Facsimile: (865)576-5728
E-Mail: reports@adonis.osti.gov
Online ordering: http://www.osti.gov/bridge

Available to the public from
U.S. Department of Commerce
National Technical Information Service
5285 Port Royal Rd
Springfield, VA 22161

Telephone: (800)553-6847
Facsimile: (703)605-6900
E-Mail: orders@ntis.fedworld.gov
Online order: http://www.ntis.gov/help/ordermethods.asp?loc=7-4-0#online

SAND2005-7246
Unlimited Release
Printed November 2005

Piezoelectric Field in Strained GaAs

Sebastian M. Wieczorek and Weng W. Chow
Semiconductor Materials and Device Sciences
Sandia National Laboratories
P.O. Box 5800
Albuquerque, New Mexico 87185-0601

Abstract

This report describes an investigation of the piezoelectric field in strained bulk GaAs. The bound charge distribution is calculated and suitable electrode configurations are proposed for (i) uniaxial and (ii) biaxial strain. The screening of the piezoelectric field is studied for different impurity concentrations and sample lengths. Electric current due to the piezoelectric field is calculated for the cases of (i) fixed strain and (ii) strain varying in time at a constant rate.

Intentionally left blank

Contents

1. Introduction 7

2. Electrode configurations 9
   2.1. Uniaxial stress or strain..... 9
   2.2. Biaxial stress or strain 11
   2.3. Comparison with previous results 13

3. Piezoelectric current 14
   3.1. Effect of doping on the total field inside the crystal 14
   3.2. Piezoelectric current for a fixed strain 17
   3.3. Generation od a DC current..... 19

4. Conclusions 21

5. References 22

Figures

Figure 1. Illustration of the stress tensor components..... 7

Figure 2. Piezoelectric field component in GaAs 8

Figure 3. Bound charges in GaAs as a result of uniaxial stress 9

Figure 4. Piezoelectric field vs. uniaxial strain and stress..... 10

Figure 5. Bound charges in GaAs as a result of biaxial stress… 11

Figure 6. Piezoelectric field vs. biaxial strain and stres..... 12

Figure 7. Bound charges and the resulting piezoelectric field in a strained crystal 14

Figure 8. The screening length as a function of carrier density for T = 0 K and T = 300 K 15

Figure 9. The screened electric as a function of the distance z from the crystal surface…..... 16

Figure 10. A setup for the piezoelectric current (undoped crystal) 17

Figure 11. Decaying current after the switch *S* in the circuit from Fig. 9 is on 18

Intentionally left blank

1. Introduction

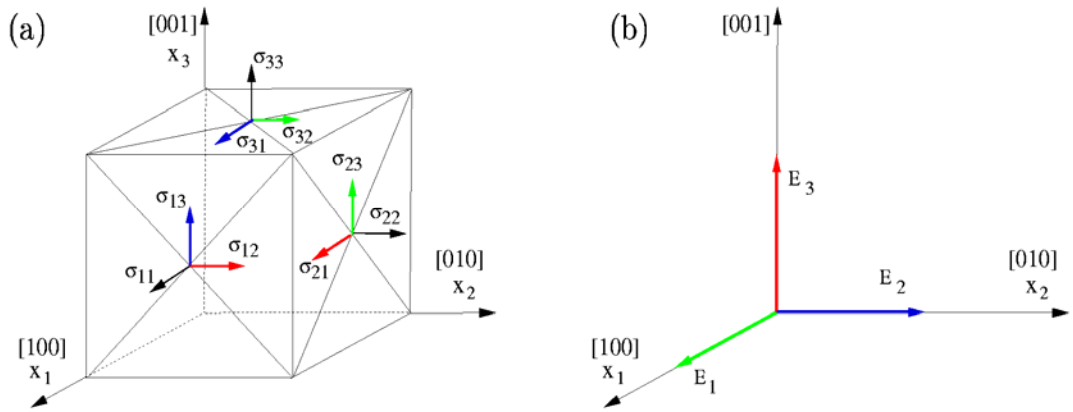

Figure 1. (a) Illustration of the stress tensor components at a point represented by an infinitesimal cube. (b) In the cubic crystal structure piezoelectric field arises due to the shear stress or strain only. The underlying stress components and the resulting piezoelectric field vectors are plotted in the same color.

The electric field inside the GaAs crystal appears under shear (off-diagonal) stress σ_{ij} or strain ε_{ij} [1, 4, 5] (MKS units)

$$E_i = -\frac{2e_{14}\varepsilon_{j\neq k}}{\varepsilon_0(1+\chi)} = -\frac{d_{14}\sigma_{j\neq k}}{\varepsilon_0(1+\chi)},$$
$$i, j, k = 1,2,3.$$

where e_{14} and d_{14} are the piezoelectric tensor coefficients, ε_0 is the permittivity of free space and $(1+\chi)$ is the low-frequency dielectric constant. For the calculations we use $e_{14} = -0.16$ C/m^2, $d_{14} = -2.69\times10^{-12}$ m/V [2, 3], $\varepsilon_0 = 8.85\times10^{-12}$ C^2/(Nm^2), where C is Coulomb, and $(1+\chi) = 13.71$ [3] so that

$$E_i(V/cm) = 2.64\times10^7 (V/cm)\varepsilon_{j\neq k}$$

$$E_i(V/cm) = 2.22(cm^2/C)\sigma_{j\neq k}(N/cm^2)$$

The breakdown field for GaAs is 3.5×10^5 V/cm [4].

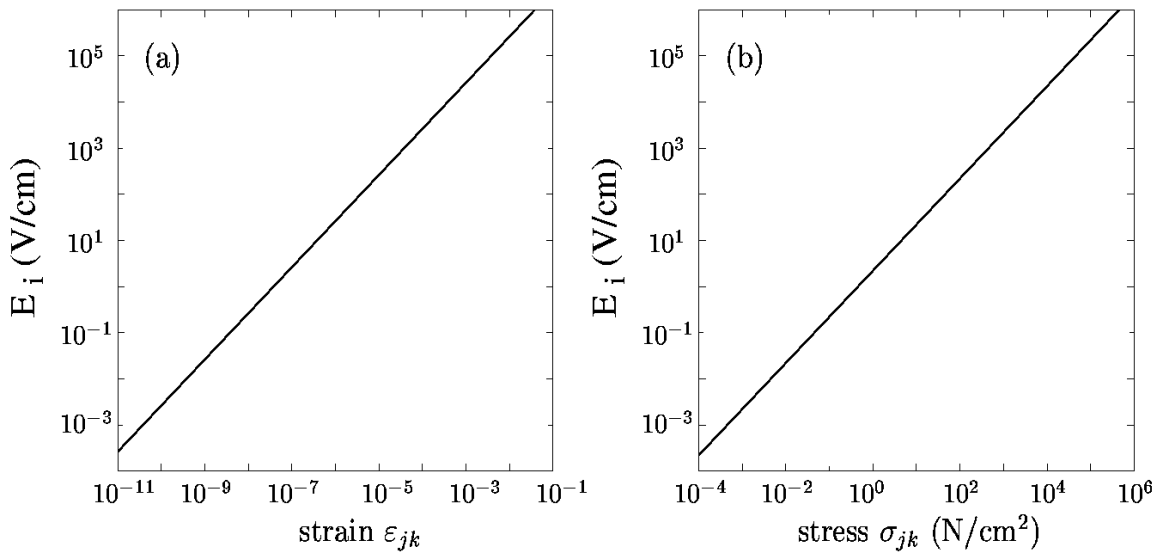

Figure 2. Piezoelectric field component in GaAs versus the off-diagonal (a) strain (deformation) component and (b) stress component.

There are three different mechanisms that contribute to the piezoelectric effect [2]: (i) the internal displacement of the ionic charge, (ii) the internal displacement of the electronic charge, and (iii) change in ionicity due to strain.

2. Electrode configurations

2.1. Uniaxial stress or strain

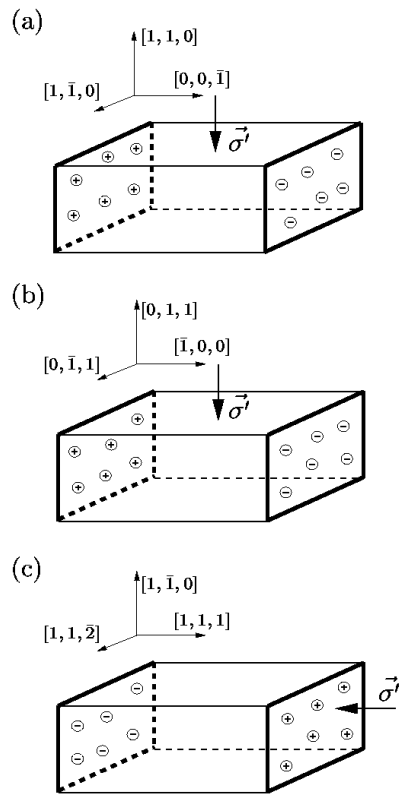

Figure 3. Bound charges in GaAs as a result of uniaxial stress applied on (a) (1,1,0) plane, (b) (0,1,1) plane, and (c) (1,1,1) plane. The thick lines denote the contacts.

These calculations are for experiments applying uniaxial stress on GaAs crystals. Uniaxial stress σ' applied on (1,1,0) plane produces piezoelectric field

$$E_{[001]} = -\frac{d_{14}\sigma'_{[110]}}{2\varepsilon_0(1+\chi)} = -\frac{e_{14}\varepsilon'_{[110]}}{\varepsilon_0(1+\chi)}$$

in [0,0,1] direction. Uniaxial stress σ' applied on (0,1,1) plane produces piezoelectric field

$$E_{[100]} = -\frac{d_{14}\sigma'_{[011]}}{2\varepsilon_0(1+\chi)} = -\frac{e_{14}\varepsilon'_{[011]}}{\varepsilon_0(1+\chi)}$$

in [1,0,0] direction. Uniaxial stress σ' applied on (1,1,1) plane produces piezoelectric field

$$E_{[111]} = -\frac{d_{14}\sigma'_{[111]}}{\sqrt{3}\varepsilon_0(1+\chi)} = -\frac{2e_{14}\varepsilon'_{[111]}}{\sqrt{3}\varepsilon_0(1+\chi)}$$

in [1,1,1] direction [2]. Figure 3 illustrates three possible electrode configurations; compare with Fig. 7 of Ref. [6].

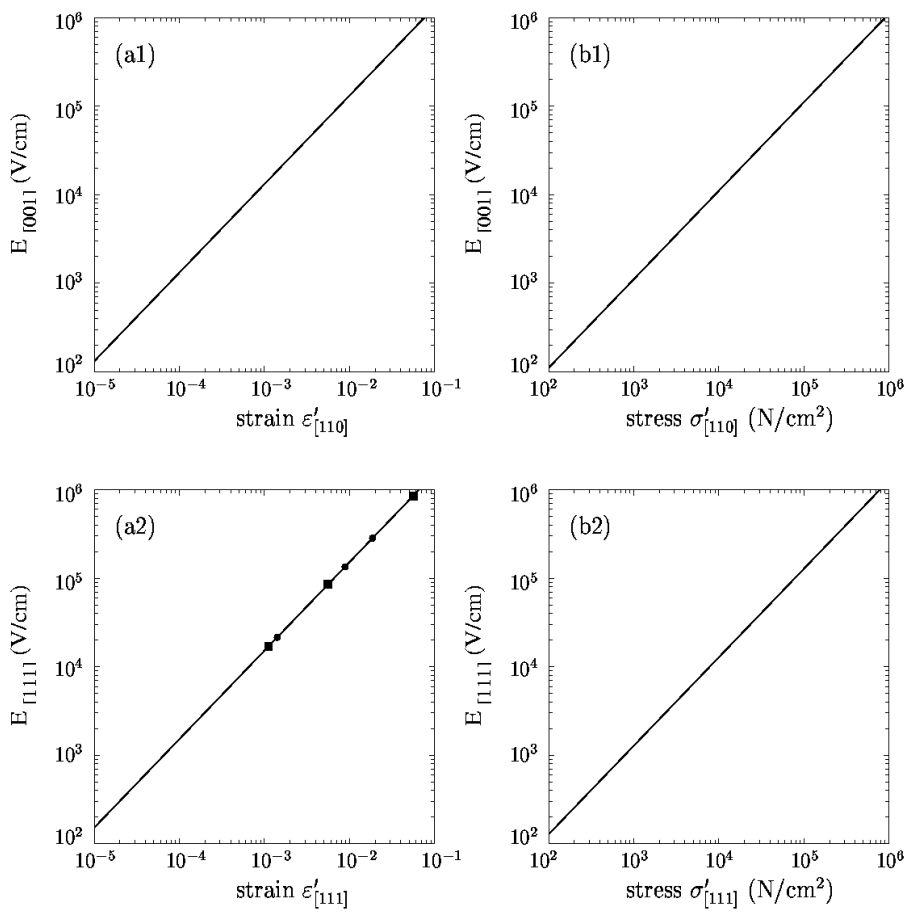

Figure 4. (top) Piezoelectric field in [0,0,1] direction vs. uniaxial (a1) strain and (b1) stress in [1,1,0] direction. (bottom) Piezoelectric field in [1,1,1] direction vs. uniaxial (a2) strain and (b2) stress in [1,1,1] direction. In panel (a2) the squares indicate theoretical results from Ref. [2] and the dots indicate theoretical results from Ref. [4].Notice that uniaxial strain in [111] direction causes the strongest piezoelectric field.

2.2. Biaxial stress or strain

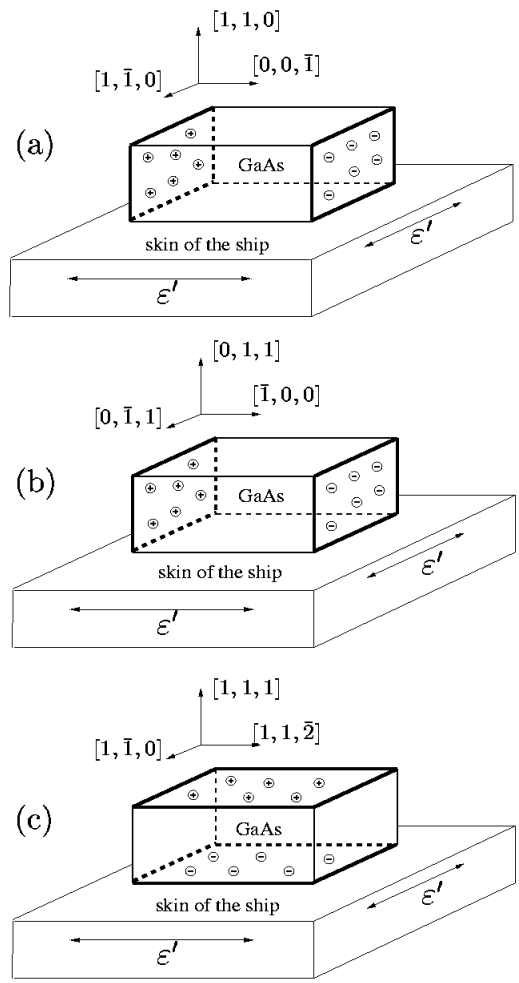

Figure 5. Bound charges in GaAs as a result of biaxial stress in (a) (1,1,0) plane, (b) (0,1,1) plane, and (c) (1,1,1) plane. The thick lines denote the contacts.

In an application, a GaAs crystal that is attached to an expanding or contracting surface experiences biaxial strain. Biaxial strain ε' in (1,1,0) plane produces piezoelectric field

$$E_{[001]} = \frac{2e_{14}}{\varepsilon_0(1+\chi)} \frac{C_{11}+C_{12}}{C_{11}+C_{12}+2C_{44}} \varepsilon',$$

in [0,0,1] direction. Biaxial strain ε' in (0,1,1) plane produces piezoelectric field

$$E_{[100]} = \frac{2e_{14}}{\varepsilon_0(1+\chi)} \frac{C_{11}+C_{12}}{C_{11}+C_{12}+2C_{44}} \varepsilon',$$

in [1,0,0] direction. Biaxial strain ε' in (1,1,1) plane produces piezoelectric field

$$E_{[111]} = \frac{2\sqrt{3}e_{14}}{\varepsilon_0(1+\chi)} \frac{C_{11}+2C_{12}}{C_{11}+2C_{12}+4C_{44}} \varepsilon',$$

in [1,1,1] direction [7]. The elastic stiffness constants C take values: $C_{11} = 11.88 \times 10^{10}$ N/m^2, $C_{12} = 5.83 \times 10^{10}$ N/m^2, and $C_{44} = 5.94 \times 10^{10}$ N/m^2. Figure 5 illustrates three possible electrode configurations for the crystal attached to a surface.

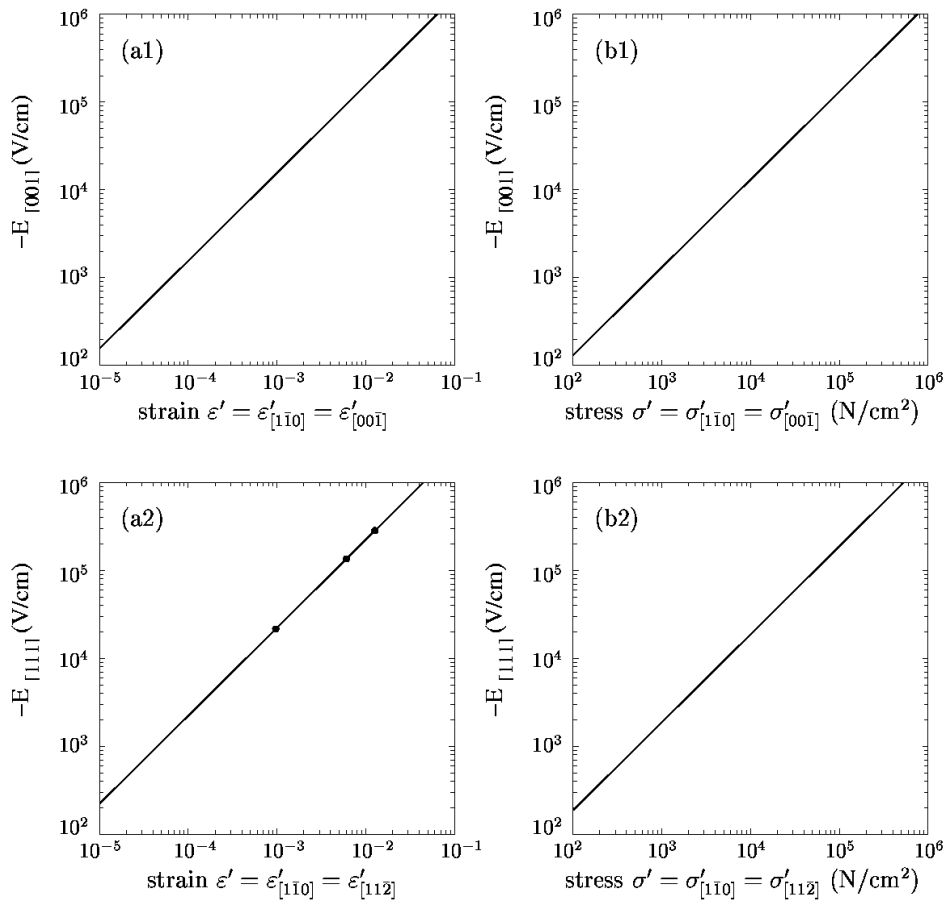

Figure 6. (top) Piezoelectric field in [0,0,1] direction vs. biaxial (a1) strain and (b1) stress in (1,1,0) plane. (bottom) Piezoelectric field in [1,1,1] direction vs. biaxial (a2) strain and (b2) stress in (1,1,1) plane. In panel (a2) the dots indicate theoretical results from Ref.~\cite{SMI86}.Notice that strain in (111) plane causes the strongest piezoelectric field.

2.3. Comparison with previous studies

The piezoelectric field $E_{[111]}$ dependence on the uniaxial strain $\varepsilon_{[111]}$ [line in Fig. 4 (a2)] agrees exactly with the calculations using (i) the formula for the piezoelectric contribution to the displacement $D_{[111]}$ and (ii) the measured value of $e_{14} = -0.16$ C/m^2 from Ref. [2]. The three points obtained from Ref. [2] are marked with squares in Fig. 4 (a2).

Reference [4] reports on [111]-growth axis strained layer superlattices GaAs--$Ga_{0.8}In_{0.2}As$. Both layers are under biaxial strain and the resulting shear strain causes piezoelectric field in [111] direction. We compared our calculations with the results from Ref. [4] and the three points obtained from Ref. [4] are marked with dots in Figs. 4 (a2) and 6 (a2).

In Ref. [7] the piezoelectric field in biaxially strained $In_{0.15}Ga_{0.85}As$ quantum well grown along [111] axis on GaAs is measured to be $2.2 \pm 0.5 \times 10^5$ V/cm. The theoretical value of 2.1×10^5 V/cm obtained with the formula

$$E_{[111]} = \frac{2\sqrt{3}e_{14}}{\varepsilon_0(1+\chi)} \frac{C_{11}+2C_{12}}{C_{11}+2C_{12}+4C_{44}} \varepsilon,$$

using parameters for $In_{0.15}Ga_{0.85}As$ is in good agreement with the measurements.

3. Piezoelectric current

3.1. Effect of doping on the total field inside the crystal

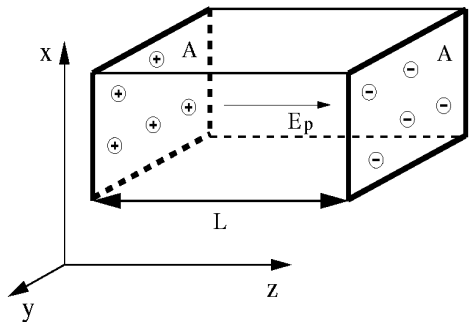

Figure 7. Bound charges and the resulting piezoelectric field in a strained crystal.

Let us assume that a GaAs crystal is under constant strain. The bound charge due to the piezoelectric effect appears on the crystal surfaces A which are L apart (Fig. 7). As a result, otherwise uniform distribution of free carriers inside the crystal is modified in such a way that the field due to the bound charges is screened. The resulting screened field E_s inside the crystal is

$$E_s(z) = E_p e^{-k_s z},$$

where the inverse screening length is [12]

$$k_s = \sqrt{\frac{e^2}{\varepsilon_0 \varepsilon_b} \frac{\partial n}{\partial \mu}},$$

where n is the free-carrier density and μ is the chemical potential. The inverse screening length can be calculated for three cases [12]:

(a) Thomas--Fermi approximation: at zero temperature (T = 0 K) $\mu = E_F$ giving

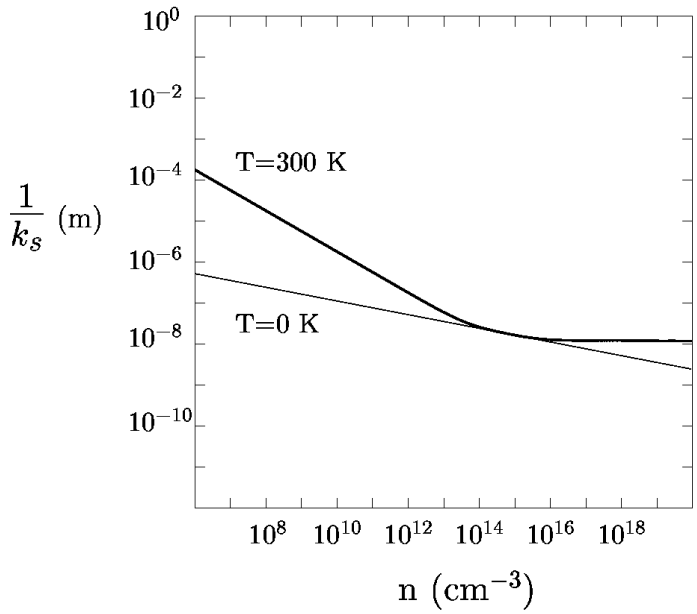

Figure 8. The screening length as a function of carrier density for T = 0 K and T = 300 K.

$$k_s^{T=0} = \sqrt{\frac{3e^2 n}{\varepsilon_0 \varepsilon_b E_F}},$$

where e is the electron charge, and $E_F = \frac{\hbar^2}{2m}(3\pi^2 n)^{2/3}$ is the Fermi energy.

(b) Debye--Huckel approximation: at very high temperatures the Fermi distribution can be approximated by the Boltzman distribution giving

$$k_s^{T>>0} = \sqrt{\frac{e^2 n}{\varepsilon_0 \varepsilon_b k_B T}},$$

where $k_B = 8 \times 10^{-23}$ J/K is the Boltzman constant and T is the temperature in Kelvins.

(c) in this report we use an analytic approximation for the chemical potential for $T > 0$

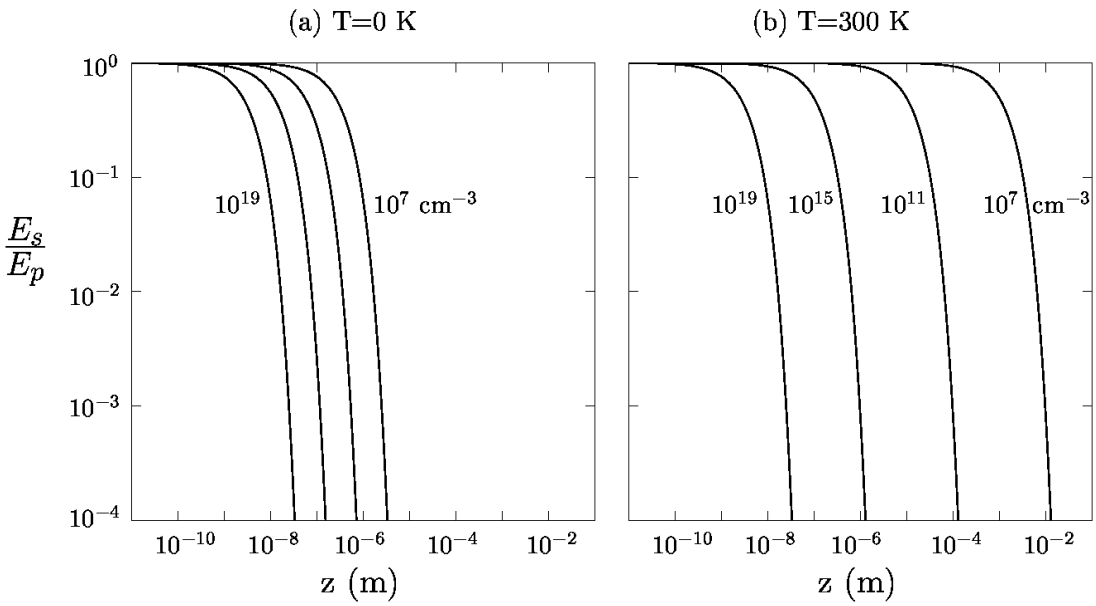

Figure 9. The screened electric field normalized with E_p as a function of the distance z from the crystal surface for (a) T = 0 K and (b) T = 300. In each panel from left to right the carrier density is $10^{19}, 10^{15}, 10^{11}$, and 10^7 cm^{-3}.

$$\mu = k_B T\left[\ln\frac{n}{n_0} + K_1 \ln\left(K_2\frac{n}{n_0}+1\right) + K_3\frac{n}{n_0}\right],$$

which is good for all situations except T near zero. Here, $K_1 = 4.897$, $K_2 = 0.045$, $K_3 = 0.133$, and $n_0 = \frac{1}{4}\left(\frac{2mk_BT}{\hbar^2\pi}\right)^{3/2}$, which gives the screening length

$$k_s = \sqrt{\frac{e^2}{\varepsilon_0\varepsilon_b k_B T\left(\frac{1}{n} + K_1\frac{1}{n+\frac{n_0}{K_2}} + K_3\frac{1}{n_0}\right)}}.$$

Notice that this formula reduces to case (b) for $K_1 = K_3 = 0$.

Figure 8 shows the dependence of the screening length on the carrier concentration and Fig. 9 shows the normalized (with respect to E_p) screened electric field inside the crystal.

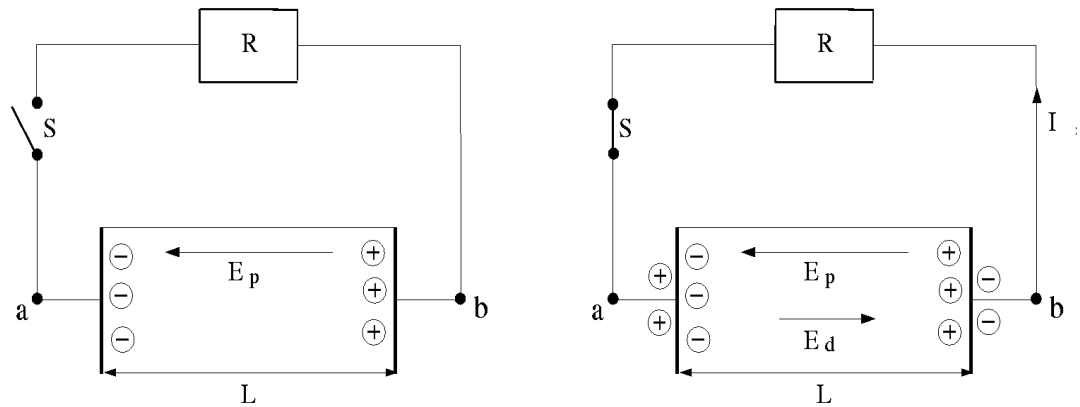

Figure 10. A setup for the piezoelectric current (undoped crystal)

Note that the screening depends on the carrier density and on the thickness of the crystal L.

In samples with $L < 10^{-4}$ m and at T 300 K, intrinsic carrier concentration of 10^{-7} cm^{-3} does not screen the piezoelectric field. However, at higher impurity densities the piezoelectric field will be screened by free carriers. For example, at $n = 10^{15}$ cm^{-3} the piezoelectric field will be reduced by three orders of magnitude for a sample length of $\approx$ 1 micron.

3.2. Piezoelectric current for a fixed strain

We now assume that a strained crystal is used in a circuit with resistance *R* [Fig. 10 (left panel)] and calculate the resulting electric current after the switch *S* in on [Fig. 10 (right panel)]. We treat the crystal as a capacitor of capacitance $C = \varepsilon A / L = q_p / V_{ab}(t = 0)$, where $q_p = \varepsilon A E_p$ is the bound charge associated with the piezoelectric field E_p. If there is no doping and the switch *S* is on at time $t = 0$, a current will result in the circuit due to the potential difference $V_{ab}(t)$ between the points a and b

$$I(t) = \frac{V_{ab}(t)}{R} = \frac{q(t)}{RC},$$

If *q* is the charge of the capacitor and *Q* is the charge flowing through the circuit then the charge conservation gives

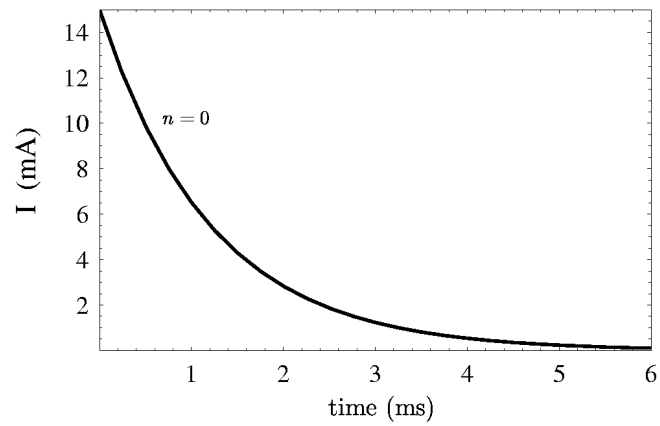

Figure 11. Decaying current after the switch *S* in the circuit from Fig. 9 is on for *n* = 0. For this figure $A = 10^{-2}$ **m**^{2}**,** $L = 10^{-3}$ **m, and** $R = 1$ **M**Ω**.**

$$I(t) = \frac{dQ}{dt} = -\frac{dq}{dt}$$

so that

$$\frac{dq}{dt} = -q\frac{1}{RC}$$

which has the solution

$$q(t) = q(0)e^{-\frac{1}{RC}t}$$

with $q(0) = q_p$. Differentiating the above equation gives the expression for the current in the circuit

$$I(t) = -\frac{dq}{dt} = \frac{q_p}{RC}e^{-\frac{1}{RC}t} = \frac{V_{ab}(t=0)}{R}e^{-\frac{1}{RC}t} = \frac{E_p L}{R}e^{-\frac{1}{RC}t}.$$

Because no work is being done on the system, there will be no DC current. However, some work have been put into straining the crystal and there will be a decaying current to discharge the capacitor. As the free charges accumulate at the electrodes the field E_d compensates the piezoelectric field E_p and the total field between the two electrodes

vanishes [Fig. 10 (right panel)]. Assuming $C = 1.2\,\text{nF}$ [$A = 10^{-2}\,\text{m}^2$, $L = 10^{-3}$ m, $\varepsilon = 13.7 \times 8.85 \times 10^{-12}\ \text{C}^2/(\text{Nm}^2)$] and R=1 MΩ we get the decay rate $RC \approx 1.2$ ms. The decaying current is plotted in Fig. 11.

If there is doping the piezoelectric field will be screened even before the switch is on. If the piezoelectric field is not completely screened by free carriers (see Fig. 9) there will be a decaying current after the switch is on

$$I(t) = \frac{E_s L}{R} e^{-\frac{1}{RC}t}$$

which is smaller than the corresponding current for undoped material ($E_s < E_p$).

3.3. Generation of a DC current

Let us assume that there is no doping. As the crystal is strained and the lattice is deformed there is a genuine motion of bound charges leading to bound-charge electric current (this is different from the free-carrier current which involves motion of free electrons). The piezoelectric field inside GaAs increases with the strain ε according to

$$\frac{dE_p}{dt} = \frac{2e_{14}}{\varepsilon_0 \varepsilon_b} \frac{d\varepsilon}{dt}.$$

Concurrently, as described in the previous section, free electrons move through the circuit to discharge the capacitor

$$\frac{dE_d}{dt} = -\frac{1}{RC}(E_d - E_p).$$

Under the assumption that the crystal is expanding (contracting) on a time scale much longer than *RC*, that is

$$\frac{dE_d}{dt} >> \frac{dE_p}{dt},$$

the field E_d adiabatically follows the changes in E_p [$E_d(t) = E_p(t)$]. Thus, on the one hand

$$\frac{dE_d}{dt} = \frac{2e_{14}}{\varepsilon_0 \varepsilon_b} \frac{d\varepsilon}{dt},$$

and on the other hand,

$$\frac{dE_d}{dt} = \frac{1}{\varepsilon_0 \varepsilon_b A} \frac{dq}{dt},$$

leading to

$$I(t) = 2e_{14} A \frac{d\varepsilon}{dt}$$

As long as work is being done on the crystal (expanding or contracting) the bound charges shift inside the crystal and there is electric current in the circuit. For a DC current the rate of change of strain should be a constant. For example, a strain increase at the rate of 1 %/h results in a DC current of 10^{-8} A during the crystal expansion (contraction).

If there is doping and the piezoelectric field is screened the total current in the circuit will be reduced.

4. Conclusions

We presented an investigation of the piezoelectric field in strained bulk GaAs. It is found that a lattice mismatch (strain) of 1% in [1,1,1] direction can give rise to piezoelectric field of $\approx 10^5$ V/m. In samples with thickness less than 10^{-4} m and at T=300 K, intrinsic carrier concentration of 10^{-7} cm^{-3} does not appear to screen the piezoelectric field. However, at higher impurity densities, for example at n= 10^{15} cm^{-3}, the piezoelectric field may be reduced by as much as three orders of magnitude for sample thickness of 1micron. If the piezoelectric field is not totally screened, a strained crystal can generate an electric current when it is connected to an electrical circuit. For a fixed strain, an exponentially decaying current will result. For a DC current the strain has to vary in time at a constant rate. For example, for intrinsic GaAs with area of 1 cm^2, a strain increase at the rate of 1%/h results in a DC current of 10^{-8}A during the crystal expansion (or contraction).

5. References

[1] G. Arlt and P. Quadflieg, ``Piezoelectricity in III-V compounds with a phenomenological analysis of the piezoelectric effect", *Phys. Stat. Sol.* **25** (1968) 323--330.

[2] S. Adachi,``GaAs, AlAs, and $Al_x Ga_{(1-x)} As$: Material parameters for use in research and device applications", *J. Appl. Phys*. **58** (1985) R1--R28.

[3] D. Smith, ``Strain-generated electric fields in [111] growth axis strained-layer superlattices", *Solid State Communications* **57** (1986) 919--921.

[4] C. Mailhiot and D. Smith, ``Effects of external stress on the electronic structure and optical properties of [001]—and [111]--growth--axis semiconductor superlattices", *Phys. Rev. B* **38** (1988) 5520--5529.

[5] K. Hjort, J. S\"oderkvist and J. Ake-schweitz, ``Gallium arsenide as a mechanical material", *Journal of Micromechanics and Microengineering* **4** (1994) 1--13.

[6] H. Shen, M. Dutta, W. Chang, R. Moerkirk, D.M. Kim, K.W. Chung, P.P. Ruden, M.I. Nathan, and M.A. Stroscio, ``Direct measurement of piezoelectric field in a [111]B grown InGaAs/GaAs heterostructure by Franz-Keldysh oscillations", *Appl. Phys. Lett*. **60** (1992) 2400--2402.

[7] N. W. Ashcroft and N. D. Mermin, *Solid State Physics*, W.B. Sounders Company (1976).

[8] P.A. Houston and G.R. Evans, ``Electron drift velocity in n-GaAs at high electric fields", *Solid State Electronics* **20** (1977) 197--204.

[9] P.M. Smith, M. Inoue, and J. Fey , ``Electron velocity in Si and GaAs at very high electric fields", *Appl. Phys. Lett.* **37** (1980) 797--798.

[10] J. S. Blakemore, ``Semiconducting and other major properties of Gallium arsenide", *J. Appl. Phys.* **53** (1982) R123--R181.

[11] H. Haugh and S. W. Koch, *Quantum Theory of the Optical and Electronic Properties of Semiconductors*, World Scientific Publishing 2004.

Distribution:

1	MS0601	Daniel Barton	1123
5	MS0601	Weng W. Chow	1123
1	MS1073	Michael R. Daily	1712
2	MS1073	James S. Foresi	1712-1
1	MS0603	James J. Hudgens	1713
5	MS0601	Sebastian Wieczorek	1123
2	MS9018	Central Technical Files	8945-1
2	MS0899	Technical Library	9616